Global Behavior of a Nonlinear Quasiperiodic Mathieu Equation

RANDOLPH S. ZOUNES
Center for Applied Mathematics, Cornell University, Ithaca, NY 14853, U.S.A.

RICHARD H. RAND
Department of Theoretical and Applied Mechanics, Cornell University, Ithaca, NY 14853, U.S.A.

Abstract. In this paper, we investigate the interaction of subharmonic resonances in the nonlinear quasiperiodic Mathieu equation,

$$\ddot{x} + [\delta + \varepsilon(\cos\omega_1 t + \cos\omega_2 t)]x + \alpha x^3 = 0. \tag{1}$$

We assume that $\varepsilon \ll 1$ and that the coefficient of the nonlinear term, α, is positive but not necessarily small. We utilize Lie transform perturbation theory with elliptic functions – rather than the usual trigonometric functions – to study subharmonic resonances associated with orbits in $2m{:}1$ resonance with a respective driver. In particular, we derive analytic expressions that place conditions on $(\delta, \varepsilon, \omega_1, \omega_2)$ at which subharmonic resonance bands in a Poincaré section of action space begin to overlap. These results are used in combination with Chirikov's overlap criterion to obtain an overview of the $\mathcal{O}(\varepsilon)$ global behavior of equation (1) as a function of δ and ω_2 with ω_1, α, and ε fixed.

Keywords: Nonlinear quasiperiodic Mathieu equation, elliptic functions, Lie transforms, resonance.

1. Introduction

In this paper, we make use of Chirikov's overlap criterion [2] and the analytic machinery presented in [7] to investigate the interaction of subharmonic resonances in the nonlinear quasiperiodic (QP) Mathieu equation,

$$\ddot{x} + [\delta + \varepsilon(\cos\omega_1 t + \cos\omega_2 t)]x + \alpha x^3 = 0. \tag{2}$$

In particular, we derive analytic expressions that place conditions on $(\delta, \varepsilon, \omega_1, \omega_2)$ at which subharmonic resonance bands in a Poincaré section of action space begin to overlap. We assume that the parametric perturbation, $\varepsilon(\cos\omega_1 t + \cos\omega_2 t)$, is small and that the coefficient of the nonlinear term, α, is positive but not necessarily small. In this case, we may set $\alpha = 1$ without loss of generality, because a rescaling of x can absorb α into the scaling coefficient.

The integrable structure of the unperturbed ($\varepsilon = 0$) Hamiltonian induced by the nonlinear QP Mathieu equation,

$$H(x, y) = \frac{1}{2}y^2 + \frac{1}{2}\delta x^2 + \frac{1}{4}\alpha x^4, \tag{3}$$

provides a framework for developing an analysis of the perturbed orbit structure. Lie transform perturbation theory is utilized to single out perturbation harmonics of the QP Hamiltonian, terms of the Hamiltonian that lead to subharmonic resonances associated with orbits in $2m{:}1$ resonance with a respective driver. The resulting Hamiltonian is then transformed to 'slow

flow' coordinates, yielding the so-called 'resonance Kamiltonian' whose level curves correspond to invariant curves of the associated Poincaré map. The resonance Kamiltonian enables one to derive analytic expressions for features of associated resonance bands in Poincaré sections of action-angle space – like the locations of bounding separatrices of resonance bands – suitable for the application of Chirikov's overlap criterion. The transformation of the unperturbed, nonlinear system to action-angle variables involves elliptic functions. Our investigation, therefore, is not restricted to a neighborhood of the origin.

Nonlinear resonances, those associated with orbits in resonance with one or both drivers, arise when the parametric perturbation is introduced into the unperturbed Hamiltonian. The phase space for the nonlinear QP Mathieu equation in action-angle coordinates, (Φ, J), is densely filled with resonance bands. They emerge from resonant tori at action values, J, that satisfy the 3-frequency resonance relation,

$$n_1 \frac{\omega_1}{\sqrt{\delta}} + n_2 \frac{\omega_2}{\sqrt{\delta}} = 2m\Omega(J), \tag{4}$$

where $\Omega(J)$ is the frequency (with respect to $\tau = \sqrt{\delta}\,t$) of the resonant orbit of the unperturbed system. Furthermore, solutions exhibit either 3-frequency QP behavior, corresponding to invariant tori not destroyed under the perturbation, or are locked within the domain of a resonance band.

The simultaneous influence of two or more perturbation harmonics of the Hamiltonian is associated with the overlap of the corresponding resonance bands. This generally leads to motion that is irregular in a large region of phase space, because the overlap of resonance bands enables trajectories to move from one resonance band to another. The prediction of such overlap can be made by applying Chirikov's overlap criterion and, accordingly, we derive analytic expressions that place conditions on $(\delta, \varepsilon, \omega_1, \omega_2)$ at which subharmonic resonance bands in a Poincaré section of action space begin to overlap.

Chirikov's overlap criterion is a heuristic scheme for estimating the size of the perturbation parameter – in this case ε – at which the transition between local and global chaos occurs in a Hamiltonian system. This is defined to occur when the two primary resonance bands in phase space first begin to overlap, or equivalently, when the respective separatrices that bound these regions first touch. Perturbation methods provide the location and size of the two primary resonance bands in phase space as a function of ε, a calculation that is performed for each resonance band independently. The critical value of ε at which the transition from local to global chaos ensues, therefore, is the value of ε at which the corresponding separatrices of two resonance regions by first touch.

We restrict the proceeding analysis to the interaction of subharmonic resonances associated with orbits in $2m$:1 or $2k$:1 resonance with a respective driver, $\cos \omega_1 t$ or $\cos \omega_2 t$, since resonances associated with a combination of driving frequencies are not visible at the $\mathcal{O}(\varepsilon)$ level of analysis. In other words, we consider only resonances that satisfy either one of the following resonance relations:

$$\frac{\omega_1}{2m\sqrt{\delta}} = \Omega(J_m), \tag{5}$$

$$\frac{\omega_2}{2k\sqrt{\delta}} = \Omega(J_k). \tag{6}$$

The interaction of the primary resonances – those associated with orbits in 2:1 resonance with either one of the two drivers – is of particular interest since resonance bands associated with higher-order resonances occupy significantly smaller regions of phase space.

We conclude this paper with a summary of the global behavior of the nonlinear QP Mathieu equation (as a function of δ and ω_2 with ω_1 set to 1 and ε fixed) and compare it to the behavior of the associated system linearized about the origin. Regions of instability[1] associated with 2:1 resonances between the respective driving frequencies and the natural frequency of the system are, to leading order, bounded by the transition curves

$$\delta = \frac{1}{4}\omega^2 \pm \frac{1}{2}\varepsilon + \mathcal{O}(\varepsilon^2) \tag{7}$$

and

$$\delta = \frac{1}{4} \pm \frac{1}{2}\varepsilon + \mathcal{O}(\varepsilon^2). \tag{8}$$

The four transition curves given by Equations (7) and (8) partition the δ-ω parameter plane into nine disjoint regions, as shown in Figure 7 at the end of this paper. We describe the behavior of solutions of the nonlinear QP Mathieu equation in each region and make general comments regarding the similarities and differences of the linear and nonlinear systems. Detailed analyses of the (linear) QP Mathieu equation can be found in [4–6, 8].

2. Transformation of Hamiltonian for Application of Lie Transforms

The idea underlying the analysis is to assume that resonance bands in phase space are sufficiently separated from one another and to restrict the analysis to a region of phase space occupied by one. This assumption implies that ω_1 and ω_2 be sufficiently separated, as well. The influence of the 'distantly' located resonance bands is assumed to be neglible compared to the influence of the resonance band in the region of analysis.

As stated above, Lie transform perturbation theory is utilized to single out perturbation harmonics of the QP Hamiltonian, terms of the Hamiltonian that lead to subharmonic resonances associated with orbits in $2m$:1 resonance with a respective driver. The resulting Hamiltonian is then transformed to 'slow flow' coordinates, yielding the resonance Kamiltonian whose level curves correspond to invariant curves of the associated Poincaré map. Before Lie transforms can be applied, the QP Hamiltonian will be transformed into action-angle coordinates – via two canonical transformations – and expanded in a Fourier series. The terms of the Fourier series are the aforementioned harmonics.

The Hamiltonian induced by the nonlinear QP Mathieu equation, upon scaling time and space according to $\tau \to \sqrt{\delta}\, t$ and $x \to \sqrt{\alpha/\delta}\, x$, may be written

$$H(x, y, \tau) = H_0(x, y) + \frac{\varepsilon}{2\delta} x^2 \left[\cos\left(\frac{\omega_1}{\sqrt{\delta}}\tau\right) + \cos\left(\frac{\omega_2}{\sqrt{\delta}}\tau\right) \right], \tag{9}$$

where x and y are canonically conjugate variables and

$$H_0(x, y) = \frac{1}{2}y^2 + \frac{1}{2}x^2 + \frac{1}{4}x^4.$$

---

[1] A region of instability is defined as the set of parameter values for which the origin is unstable.

Executing the sequence of canonical transformations,

$$(x, y) \rightarrow (\Phi, J),$$

$$(\Phi, J) \rightarrow (\phi, j),$$

given by

$$x(J, \Phi) = X_0(J) \operatorname{cn}\left(4K(k)\frac{\Phi}{2\pi}, k\right),$$

$$y(J, \Phi) = -X_0(J)\sqrt{1 + X_0^2} \operatorname{sn}\left(4K(k)\frac{\Phi}{2\pi}, k\right) \operatorname{dn}\left(4K(k)\frac{\Phi}{2\pi}, k\right)$$

and

$$J(j) = \frac{2}{3}\sqrt{1 + 2j}\left(-\tilde{E}(j) + (1 + j)\tilde{K}(j)\right),$$

$$\Phi(j, \phi) = \frac{\phi}{\sqrt{1 + 2j}\,\tilde{K}(j)},$$

puts the Hamiltonian in terms of the action-angle coordinates (ϕ, j); details of the derivation of these two canonical transformations can be referenced in [6] or [7]. The terms $\tilde{E}(j) \equiv 2E\big(k(j)\big)/\pi$ and $\tilde{K}(j) \equiv 2K\big(k(j)\big)/\pi$ are the normalized, complete elliptic integrals of the first kind as functions of j; k is the elliptic modulus. The elliptic modulus is usually determined by initial conditions, and in this case, k is explicitly defined in terms of the amplitude of motion, $x(0) = X_0$. When viewed as a function of j, $k(j)$ satisfies

$$k^2 \stackrel{\text{def}}{=} \frac{\frac{1}{2}X_0^2}{1 + X_0^2} = \frac{j}{1 + 2j}.$$

The transformed Hamiltonian in the (ϕ, j) coordinate system is, thus,

$$H(\phi, j, \tau) = j + j^2 + \varepsilon\,H_1(\phi, j, \tau),$$

where

$$\varepsilon\,H_1(\phi, j, \tau) = \frac{\varepsilon}{\delta}\,j\operatorname{cn}^2\left(\frac{\tilde{K}(j)}{J'(j)}\phi, k\right)\left[\cos\left(\frac{\omega_1}{\sqrt{\delta}}\tau\right) + \cos\left(\frac{\omega_2}{\sqrt{\delta}}\tau\right)\right] \qquad (10)$$

and $J'(j) = dJ/dj$ is defined via the canonical transformation, $(\Phi, J) \rightarrow (\phi, j)$.

The final step of this procedure is the expansion of the Hamiltonian (or more precisely the elliptic function cn) in a Fourier series. When expressed as a sum of trigonometric terms, Lie transform perturbation theory becomes directly applicable: individual harmonics leading to resonance bands in phase space are explicitly identified.

The representation of the cn function as a Fourier series is given in [1] by Byrd and Friedman:

$$\operatorname{cn}(u, k) = \frac{2\pi}{kK}\sum_{n=0}^{\infty} g_n(k)\cos\left[(2n + 1)\frac{\pi u}{2K}\right], \qquad (11)$$

where

$$g_n(k) = \frac{1}{2} \operatorname{sech}\left[\left(n + \frac{1}{2}\right)\pi\frac{K'}{K}\right],$$

$K \equiv K(k)$, and $K' \equiv K(\sqrt{1 - k^2})$. For the problem at hand, the expression for cn in the (ϕ, j) coordinate system with the arguments given in Equation (10) becomes

$$\operatorname{cn}\left(\frac{\tilde{K}(j)}{J'(j)}\phi, k\right) = \sum_{n=0}^{\infty} G_n(j) \cos\left[(2n + 1)\frac{\phi}{J'(j)}\right],$$

where the new coefficient, G_n, is defined by

$$G_n(j) = \frac{2\pi}{k(j)K(k(j))} g_n(k(j)) = \frac{4}{k(j)\tilde{K}(j)} g_n(k(j)). \tag{12}$$

Note that G_n decreases roughly exponentially with increasing n. Squaring the above expansion for cn, reducing trigonometric terms, and collecting harmonics, we obtain

$$\operatorname{cn}^2\left(\frac{\tilde{K}(j)}{J'(j)}\phi, k\right) = \mathcal{G}_0(j) + \sum_{m=1}^{\infty} \mathcal{G}_m(j) \cos\left(\frac{2m\phi}{J'(j)}\right), \tag{13}$$

where

$$\mathcal{G}_0 = \frac{1}{2}(G_0^2 + G_1^2 + G_2^2 + G_3^2 + \cdots) \sim \frac{1}{2} - \frac{1}{16}j + \frac{3}{32}j^2,$$

$$\mathcal{G}_1 = \frac{1}{2}G_0^2 + G_0G_1 + G_1G_2 + G_2G_3 + \cdots \sim \frac{1}{2} - \frac{3}{512}j^2,$$

$$\mathcal{G}_2 = G_0G_1 + G_0G_2 + G_1G_3 + G_2G_4 + \cdots \sim \frac{1}{16}j - \frac{3}{32}j^2,$$

$$\vdots$$

Inserting this result into the above Hamiltonian and reducing trigonometric terms, we obtain our sought-after result. The expanded Hamiltonian in the (ϕ, j) coordinate system is found to be,

$$H(\phi, j, \tau) = j + j^2 + \varepsilon H_1(\phi, j, \tau), \tag{14}$$

where

$$\varepsilon H_1(\phi, j, \tau) = \frac{\varepsilon}{\delta} j\mathcal{G}_0(j)\left[\cos\left(\frac{\omega_1}{\sqrt{\delta}}\tau\right) + \cos\left(\frac{\omega_2}{\sqrt{\delta}}\tau\right)\right]$$

$$+ \frac{\varepsilon}{2\delta} j \sum_{m=1}^{\infty} \mathcal{G}_m(j)\left[\cos\left(\frac{2m\phi}{J'(j)} + \frac{\omega_1}{\sqrt{\delta}}\tau\right) + \cos\left(\frac{2m\phi}{J'(j)} - \frac{\omega_1}{\sqrt{\delta}}\tau\right)\right]$$

$$+ \frac{\varepsilon}{2\delta} j \sum_{k=1}^{\infty} \mathcal{G}_k(j)\left[\cos\left(\frac{2k\phi}{J'(j)} + \frac{\omega_2}{\sqrt{\delta}}\tau\right) + \cos\left(\frac{2k\phi}{J'(j)} - \frac{\omega_2}{\sqrt{\delta}}\tau\right)\right]$$

in a form suitable for the direct application of Lie transform perturbation theory.

3. Application of Lie Transforms

Without loss of generality, we shall focus our analysis on the resonance band associated with subharmonic periodic orbits in $2m{:}1$ resonance with the first driver; i.e., restrict j to a neighborhood of j_m for which $\omega_1/2m\sqrt{\delta} = \Omega(j_m)$. The analysis for resonance bands associated with subharmonic periodic orbits in resonance with the second driver is identical. As outlined in [7], a Lie-generating function $W = W_1 + \mathcal{O}(\varepsilon)$ can be found so that the near-identity canonical transformation $(\phi, j) \to (Q, P)$,

$$\phi = Q + \varepsilon \frac{\partial W_1}{\partial P} + \mathcal{O}(\varepsilon^2),$$

$$j = P - \varepsilon \frac{\partial W_1}{\partial Q} + \mathcal{O}(\varepsilon^2),$$

yields the following Kamiltonian valid only in a neighborhood of the resonance band under investigation in the (Q, P) coordinate system:

$$K(Q, P, \tau) = P + P^2 + \frac{\varepsilon}{2\delta} P g_m(P) \cos\left(\frac{2mQ}{J'(P)} - \frac{\omega_1}{\sqrt{\delta}}\tau\right) + \mathcal{O}(\varepsilon^2). \tag{15}$$

The Lie generating function $W = W_1 + \mathcal{O}(\varepsilon)$ defining the corresponding canonical transformation is

$$
\begin{aligned}
W_1(Q, P, \tau) =\ & \frac{P g_0(P)}{\sqrt{\delta}} \left[\frac{\sin\left(\frac{\omega_1}{\sqrt{\delta}}\tau\right)}{\omega_1} + \frac{\sin\left(\frac{\omega_2}{\sqrt{\delta}}\tau\right)}{\omega_2} \right] \\
& + \frac{P}{2\sqrt{\delta}} \sum_{n=1}^{\infty}{}' g_n(P) \left[\frac{\sin\left(\frac{2nQ}{J'(P)} + \frac{\omega_1}{\sqrt{\delta}}\tau\right)}{\omega_1 + 2n\sqrt{\delta}\,\Omega(P)} - \frac{\sin\left(\frac{2nQ}{J'(P)} - \frac{\omega_1}{\sqrt{\delta}}\tau\right)}{\omega_1 - 2n\sqrt{\delta}\,\Omega(P)} \right] \\
& + \frac{P}{2\sqrt{\delta}} \sum_{k=1}^{\infty} g_k(P) \left[\frac{\sin\left(\frac{2kQ}{J'(P)} + \frac{\omega_2}{\sqrt{\delta}}\tau\right)}{\omega_2 + 2k\sqrt{\delta}\,\Omega(P)} - \frac{\sin\left(\frac{2kQ}{J'(P)} - \frac{\omega_2}{\sqrt{\delta}}\tau\right)}{\omega_2 - 2k\sqrt{\delta}\,\Omega(P)} \right],
\end{aligned}
$$

where the prime indicates that $n \neq m$. Finally, the time dependence in the Kamiltonian (15) is removed by performing the canonical transformation $(Q, P) \to (\psi, Y)$ defined by

$$P = Y,$$

$$Q = \psi + \frac{\omega_1}{2m\sqrt{\delta}} J'(Y)\,\tau.$$

The transformed Kamiltonian in the (ψ, Y) coordinate system takes the form, up to $\mathcal{O}(\varepsilon^2)$,

$$K_r(\psi, Y) = Y + Y^2 - \frac{\omega_1}{2m\sqrt{\delta}} J(Y) + \frac{\varepsilon}{2\delta} Y g_m(Y) \cos\left(\frac{2m\psi}{J'(Y)}\right). \tag{16}$$

In the new coordinate system, the transformed Kamiltonian $K_r(\psi, Y)$ does not depend explicitly on time and, therefore, remains constant. This means that the system is conservative and, hence, integrable. We refer to K_r as the *resonance Kamiltonian* since we can infer the
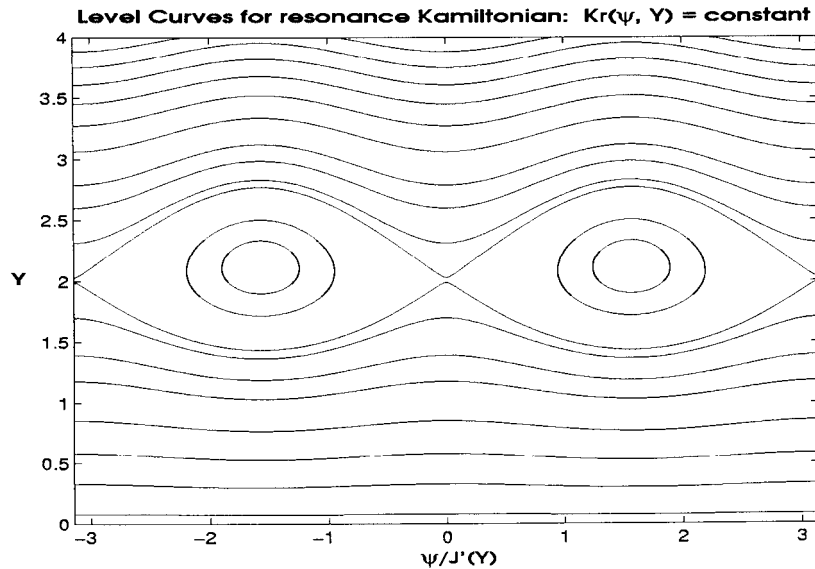
Figure 1. Level curves of the resonance Kamiltonian, K_r, as seen in the ψ-Y plane. The resonance band is bounded by action values, $Y \approx 1.4$ and $Y \approx 2.8$.

dynamics of the original system only for action values near and within the resonance band associated with $2m$:1 subharmonic periodic orbits.

Transforming back to the original (x, y) coordinates, level curves of K_r correspond to invariant curves of a Poincaré map induced by solutions of the nonlinear QP Mathieu equation (2). For example, Figure 1 presents the level curves of K_r in the ψ-Y plane for $m = 1$. The resonance band is bounded by action values, $Y \approx 1.4$ and $Y \approx 2.8$, and possesses two centers and two saddle points.

If transformed back to (x, y) coordinates, this band is mapped into the elliptical annulus centered at the origin in the $x-y$ plane. The Poinaré map shown in Figure 2 illustrates schematically the predicted result of such a transformation. It was generated by numerically integrating the nonlinear QP Mathieu equation utilizing the Dynamical System Toolkit, 'dstool' [3].

4. Overlap of Resonance Bands

In this section, we apply Chirikov's overlap criterion to derive analytic expressions that place conditions on $(\delta, \varepsilon, \omega_1, \omega_2)$ at which subharmonic resonance bands in a Poincaré section of action space begin to overlap. This generally leads to motion that is quite irregular in a large region of phase space. Overlap begins when the separatrices of the slow-flow described by K_r first touch. Our aim is to find the critical value of ε, denoted ε_c, given δ, ω_1, and ω_2, which estimates the onset of overlap.

Chirikov acknowledges that the overlap criterion provides only rough, overestimates for ε_c and states the following reasons for any discrepancies:

- Although the phase space is densely filled with resonance bands, the first-order approximation for the onset of overlap accounts for only the overlap of the two primary resonance bands. As ε is increased, resonance bands associated with high-order harmon-
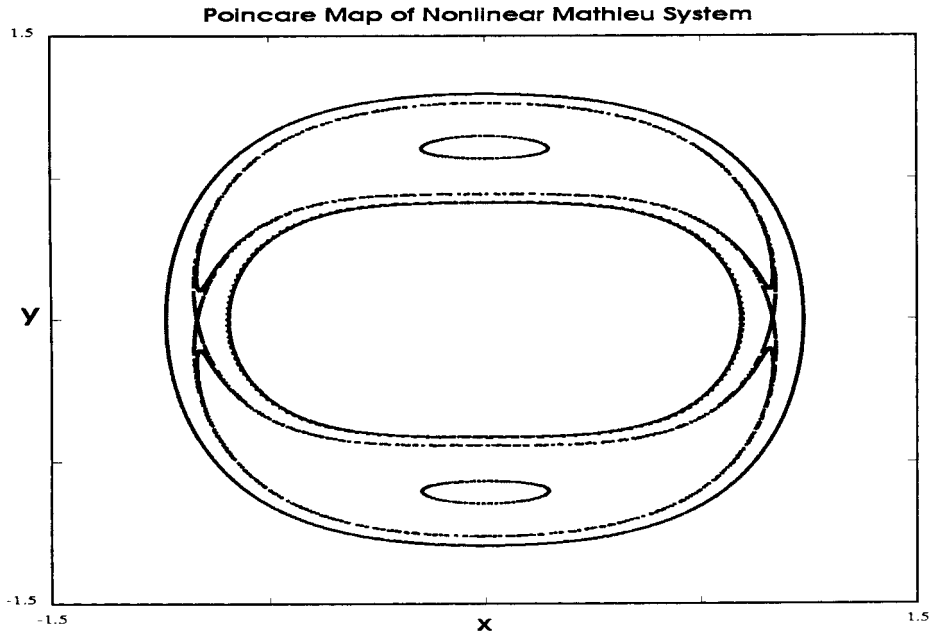
Figure 2. Schematic figure relating Figure 1, level curves of the resonance Kamiltonian in action-angle space, to the flow in the original (x, y) coordinates via a Poincaré map.

ics, located between the two primary ones, occupy increasing regions of phase space and, hence, facilitate the overlap.

- The overlap criterion ignores the mutual interaction of resonances since each corresponding resonance band is examined independently. As discussed in [2, section 5.1], separatrices become distorted as the resonance bands approach one another in phase space.

- Finally, the finite width of the separatrix layers is not taken into account. The analysis involving the resonance Kamiltonian treats the bounding separatrices as curves with no 'thickness'.

We shall now proceed with the application of Chirikov's overlap criterion to find the critical value of ε for which the two primary resonance bands begin to overlap. In order to facilitate the analysis, the following notation is used:

- $RB_{\omega_1}(2:1)$ denotes the resonance band associated with subharmonic periodic orbits in 2:1 resonance with the $\cos \omega_1 t$ driver, $RB_{\omega_2}(2:1)$ denotes the resonance band associated with subharmonic periodic orbits in 2:1 resonance with the $\cos \omega_2 t$ driver, and $RB_{\omega_2}(4:1)$ denotes the resonance band associated with subharmonic periodic orbits in 4:1 resonance with the $\cos \omega_2 t$ driver.

- The resonance band $RB_{\omega_1}(2:1)$ emerges from a resonant torus at an action value, Y_1, that satisfies the resonance relation,

$$\frac{\omega_1}{2\sqrt{\delta}} = \Omega(Y_1), \tag{17}$$

$RB_{\omega_2}(2{:}1)$ emerges from a resonant torus at an action value, Y_2, that satisfies the resonance relation,

$$\frac{\omega_2}{2\sqrt{\delta}} = \Omega(Y_2), \tag{18}$$

and $RB_{\omega_2}(4{:}1)$ emerges from a resonant torus at an action value, Y_4, that satisfies the resonance relation,

$$\frac{\omega_2}{4\sqrt{\delta}} = \Omega(Y_4). \tag{19}$$

- The resonance band is bounded by separatrices with minimum and maximum action values, respectively. The maximum action value acquired by $RB_{\omega_1}(2{:}1)$ is denoted by $Y_1^{\max}$, and the minimum action value acquired by $RB_{\omega_2}(2{:}1)$ is denoted by $Y_2^{\min}$.

4.1. CASE 1: OVERLAP OF RESONANCE BANDS $RB_{\omega_1}(2{:}1)$ AND $RB_{\omega_2}(2{:}1)$

Without loss of generality, assume $\omega_1 < \omega_2$ and fix δ. Since $\Omega(Y)$ is an increasing function of Y, it follows that $Y_1 < Y_2$, and as dictated by the overlap criterion, the separatrices bounding the primary resonance bands first touch when the parameters of the system satisfy

$$Y_1^{\max} = Y_2^{\min}.$$

Equations for the minimum and maximum action values acquired by a bounding separatrix are derived in [7] and are given by

$$Y_{\min} = Y_m - \sqrt{\frac{Y_m \, \mathcal{G}_m(Y_m)}{\delta \left(1 - \frac{\omega}{4m\sqrt{\delta}} J''(Y_m)\right)} \, \varepsilon} + \mathcal{O}(\varepsilon) \tag{20}$$

and

$$Y_{\max} = Y_m + \sqrt{\frac{Y_m \, \mathcal{G}_m(Y_m)}{\delta \left(1 - \frac{\omega}{4m\sqrt{\delta}} J''(Y_m)\right)} \, \varepsilon} + \mathcal{O}(\varepsilon). \tag{21}$$

Substituting in $m = 1$ and $\mathcal{G}_1 = 1/2$,

$$Y_1^{\max} = Y_1 + \sqrt{\frac{Y_1 \, \varepsilon}{2\delta \left(1 - \frac{\omega_1}{4\sqrt{\delta}} J''(Y_1)\right)}},$$

$$Y_2^{\min} = Y_2 - \sqrt{\frac{Y_2 \, \varepsilon}{2\delta \left(1 - \frac{\omega_2}{4\sqrt{\delta}} J''(Y_2)\right)}},$$

and setting the resulting expressions for $Y_1^{\max}$ and $Y_2^{\min}$ equal, we obtain the following approximation, ε_{12}, to the critical value, ε_c, for the onset of the overlap of $RB_{\omega_1}(2{:}1)$ and $RB_{\omega_2}(2{:}1)$:

$$\sqrt{\frac{\varepsilon_{12}}{\delta}} = \frac{Y_2 - Y_1}{\sqrt{\frac{Y_2/2}{1 - \frac{\omega_2}{4\sqrt{\delta}} J''(Y_2)}} + \sqrt{\frac{Y_1/2}{1 - \frac{\omega_1}{4\sqrt{\delta}} J''(Y_1)}}}. \tag{22}$$

To test the accuracy of the estimate ε_{12}, consider the case for which $\delta = 0.20$, $\omega_1 = 1$, and $\omega_2 = 1.65$. For these parameter values, the resonance bands $RB_{\omega_1}(2{:}1)$ and $RB_{\omega_2}(2{:}1)$ emerge from resonant tori located at the action values

$$Y_1 = 0.168078,$$

$$Y_2 = 1.651838,$$

respectively. Substituting Y_1 and Y_2 into Equation (22), the corresponding estimate for the critical value of ε is

$$\varepsilon_{12} = 0.135.$$

Performing numerical experiments with dstool by which numerically generated solutions are strobed at times $t_n = n2\pi/\omega_1$ and $t_n = n2\pi/\omega_2$, the actual critical value of ε is found to be approximately

$$\varepsilon_c^* = 0.085,$$

predictably lower than the estimates given above but of the same order of magnitude.

Figures 3 and 4 illustrate the growth and overlap of the primary resonance bands for increasing ε. For fixed parameter values $\delta = 0.20$, $\omega_1 = 1$, and $\omega_2 = 1.65$, dstool is utilized to numerically generate Poincaré maps for the nonlinear QP Mathieu equation in the $(x, \dot{x})$ phase space. The resonance bands – occupying elliptical, annular regions in phase space – are displayed on the same set of axes, although $RB_{\omega_1}(2{:}1)$ is produced by strobing the numerically generated solutions at times $t_n = n2\pi/\omega_1$, and $RB_{\omega_2}(2{:}1)$ is produced by strobing the solutions at times, $t_n = n2\pi/\omega_2$. The onset of overlap is readily apparent. Before the two resonance bands overlap, orbits remain confined to their respective resonance band. However, when $\varepsilon \geq \varepsilon_c$, orbits with initial conditions in $RB_{\omega_1}(2{:}1)$ eventually 'leak out' and iterate into the region of phase space occupied by $RB_{\omega_2}(2{:}1)$.

4.2. CASE 2: OVERLAP OF RESONANCE BANDS $RB_{\omega_1}(2{:}1)$ AND $RB_{\omega_2}(2{:}1)$ FACILITATED BY $RB_{\omega_2}(4{:}1)$

Without loss of generality, assume $\omega_1 < \omega_2$ and fix δ. The resonance band associated with subharmonic periodic orbits in 4:1 resonance with the $\cos \omega_2 t$ driver, $RB_{\omega_2}(4{:}1)$, will occupy a region of phase space between $RB_{\omega_1}(2{:}1)$ and $RB_{\omega_2}(2{:}1)$ whenever $Y_1 < Y_4 < Y_2$. Since $\Omega(Y)$ is an increasing function of Y, this situation occurs precisely when

$$\Omega(Y_1) < \Omega(Y_4) < \Omega(Y_2),$$

or equivalently,

$$\omega_1 < \frac{1}{2}\omega_2 < \omega_2.$$

Under these conditions, $RB_{\omega_2}(4{:}1)$ may facilitate the overlap of the primary resonance bands, $RB_{\omega_1}(2{:}1)$ and $RB_{\omega_2}(2{:}1)$. That is, if $RB_{\omega_2}(4{:}1)$ overlaps with $RB_{\omega_1}(2{:}1)$ and $RB_{\omega_2}(2{:}1)$ at $\varepsilon = \varepsilon_{14}$ and $\varepsilon = \varepsilon_{42}$, respectively, and if $RB_{\omega_1}(2{:}1)$ overlaps with $RB_{\omega_2}(2{:}1)$ at $\varepsilon = \varepsilon_{12}$, then

$$\varepsilon_{142} \equiv \max\{\varepsilon_{14}, \varepsilon_{42}\} \leq \varepsilon_{12}. \tag{23}$$

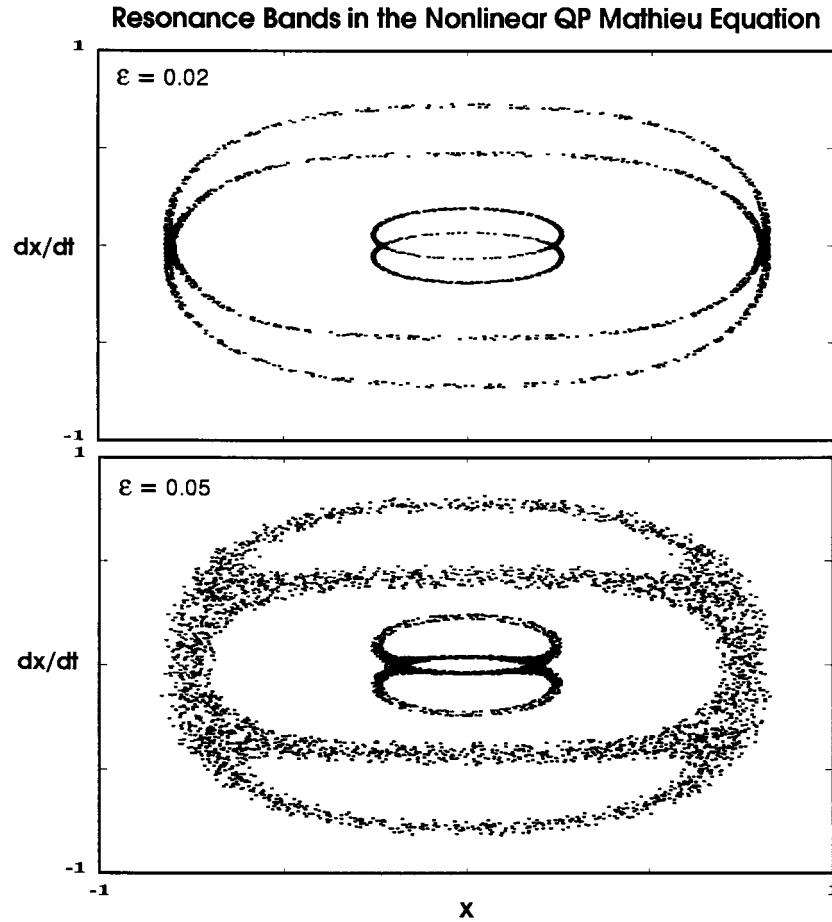**Resonance Bands in the Nonlinear QP Mathieu Equation**

Figure 3. Growth of the primary resonance bands in the nonlinear QP Mathieu equation for $\delta = 0.20$, $\omega_1 = 1$, and $\omega_2 = 1.65$. The numerically generated solutions are strobed at times $t_n = n2\pi/\omega_1$ and $t_n = n2\pi/\omega_2$ for orbits with intial conditions in $RB_{\omega_1}(2{:}1)$ and $RB_{\omega_2}(2{:}1)$, respectively. Figure 4 displays the overlap of resonance bands as ε is further increased.

More precisely, ε_{14} is defined by the relation

$$Y_1^{\max} = Y_4^{\min},$$

and ε_{42} is defined by the relation

$$Y_4^{\max} = Y_2^{\min},$$

where expressions for $Y^{\min}$ and $Y^{\max}$ are obtained by equations (20) and (21). Noting that $\mathcal{G}_1 = 1/2$ and $\mathcal{G}_2 = Y/16$, and following an analysis similiar to the one given in Case 1, we find the following expressions for ε_{14} and ε_{42}:

$$\sqrt{\frac{\varepsilon_{14}}{\delta}} = \frac{Y_4 - Y_1}{\sqrt{\frac{Y_4^2/16}{1 - \frac{\omega_2}{8\sqrt{\delta}} J''(Y_4)}} + \sqrt{\frac{Y_1/2}{1 - \frac{\omega_1}{4\sqrt{\delta}} J''(Y_1)}}} \tag{24}$$

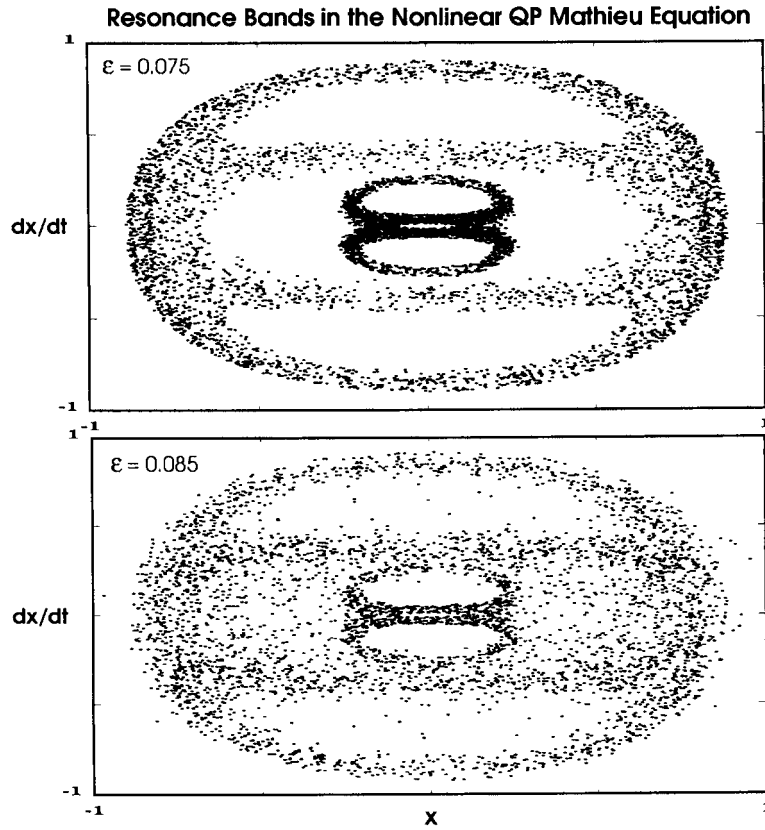**Resonance Bands in the Nonlinear QP Mathieu Equation**

Figure 4. Growth and overlap of the primary resonance bands in the nonlinear QP Mathieu equation for $\delta = 0.20$, $\omega_1 = 1$, and $\omega_2 = 1.65$. The numerically generated solutions are strobed at times $t_n = n2\pi/\omega_1$ and $t_n = n2\pi/\omega_2$ for orbits with intial conditions in $RB_{\omega_1}(2{:}1)$ and $RB_{\omega_2}(2{:}1)$, respectively.

and

$$\sqrt{\frac{\varepsilon_{42}}{\delta}} = \frac{Y_2 - Y_4}{\sqrt{\dfrac{Y_2/2}{1-\frac{\omega_2}{4\sqrt{\delta}} J''(Y_2)}} + \sqrt{\dfrac{Y_4^2/16}{1-\frac{\omega_2}{8\sqrt{\delta}} J''(Y_4)}}}. \tag{25}$$

To test the accuracy of the estimates for ε_c as determined by equations (23), (24), and (25), consider the case for which $\delta = 0.20$, $\omega_1 = 1$, and $\omega_2 = 2.55$. For these parameter values, the resonance bands $RB_{\omega_1}(2{:}1)$, $RB_{\omega_2}(4{:}1)$, and $RB_{\omega_2}(2{:}1)$ emerge from resonant tori located at the action values,

$$Y_1 = 0.168078,$$

$$Y_4 = 0.703178,$$

$$Y_2 = 4.937229,$$

respectively. Substituting Y_1, Y_4, and Y_2 into Equations (24) and (25), we find

$$\varepsilon_{14} = 0.128,$$

$$\varepsilon_{42} = 0.586,$$

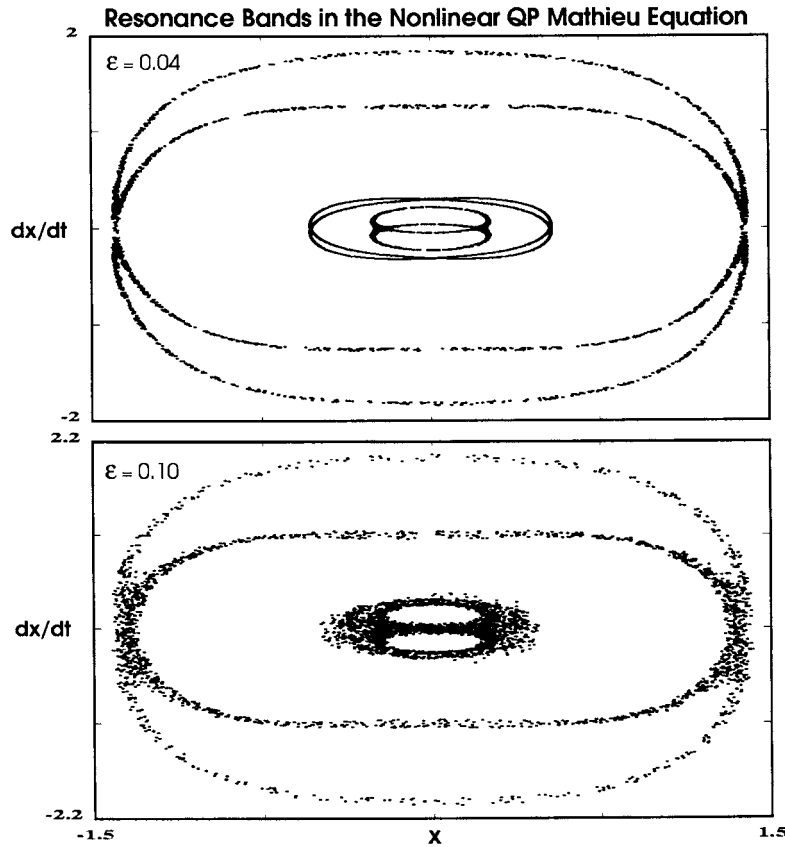**Resonance Bands in the Nonlinear QP Mathieu Equation**

Figure 5. Growth of the primary resonance bands in the nonlinear QP Mathieu equation facilitated by $RB_{\omega_2}(4{:}1)$ with $\delta = 0.20$, $\omega_1 = 1$, and $\omega_2 = 2.55$. The numerically generated solutions are strobed at times $t_n = n2\pi/\omega_1$ and $t_n = n2\pi/\omega_2$ for orbits with intial conditions in $RB_{\omega_1}(2{:}1)$ and either $RB_{\omega_2}(4{:}1)$ or $RB_{\omega_2}(2{:}1)$, respectively. Figure 6 displays the overlap of resonance bands as ε is further increased.

implying that

$$\varepsilon_{142} = 0.586.$$

Had we used Equation (22) from Case 1 for determining an estimate for ε_c, we would find that the two primary resonance bands are predicted to touch when

$$\varepsilon_{12} = 0.611,$$

indicating that the resonance band $RB_{\omega_2}(4{:}1)$ facilitates their overlap. Performing numerical experiments with dstool, we discover that the actual critical value of ε is approximately

$$\varepsilon_c^* = 0.250,$$

again, predictably lower than the estimates given above. See Figures 5 and 6 for a graphical summary of the numerical results.

We should remark that if $\omega_1 \approx \omega_2/2$, it follows that $Y_1 \approx Y_4$, and the influence of $RB_{\omega_2}(4{:}1)$ on the overlap of the primary bands becomes neglible. In this case, $RB_{\omega_1}(2{:}1)$ apparently engulfs $RB_{\omega_2}(4{:}1)$ before $RB_{\omega_2}(4{:}1)$ overlaps with $RB_{\omega_2}(2{:}1)$. For example, with
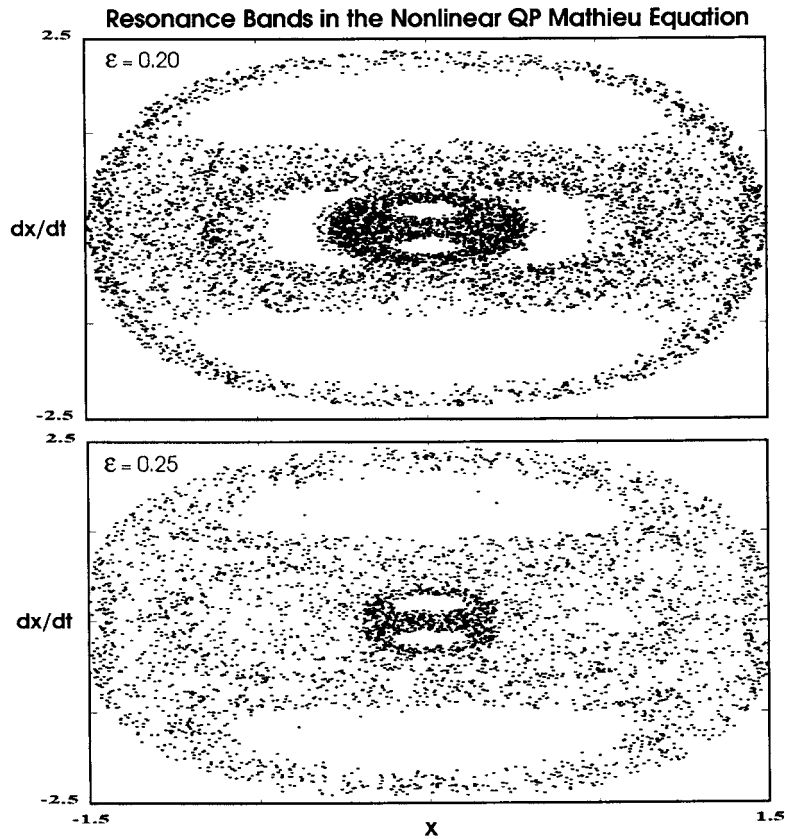
Figure 6. Growth and overlap of the primary resonance bands in the nonlinear QP Mathieu equation facilitated by $RB_{\omega_2}(4:1)$ with $\delta = 0.20$, $\omega_1 = 1$, and $\omega_2 = 2.55$. The numerically generated solutions are strobed at times $t_n = n2\pi/\omega_1$ and $t_n = n2\pi/\omega_2$ for orbits with initial conditions in $RB_{\omega_1}(2:1)$ and either $RB_{\omega_2}(4:1)$ or $RB_{\omega_2}(2:1)$, respectively.

parameter values $\delta = 0.05$, $\omega_1 = 1$, and $\omega_2 = 2.15$, the resonance bands $RB_{\omega_1}(2:1)$, $RB_{\omega_2}(4:1)$, and $RB_{\omega_2}(2:1)$ emerge from resonant tori located at the action values

$$Y_1 = 2.76,$$

$$Y_4 = 3.30,$$

$$Y_2 = 15.37,$$

respectively. Substituting Y_1, Y_4, and Y_2 into Equations (24) and (25), we find

$$\varepsilon_{14} = 0.002,$$

$$\varepsilon_{42} = 0.302,$$

implying that

$$\varepsilon_{142} = 0.302.$$

Had we used Equation (22) from Case 1 for determining an estimate for ε_c, we would find that the two primary resonance bands touch when

$$\varepsilon_{12} = 0.248;$$

i.e., our analysis predicts that $RB_{\omega_2}(4{:}1)$ does not facilitate the overlap of $RB_{\omega_1}(2{:}1)$ and $RB_{\omega_2}(2{:}1)$.

5. Summary of Global Behavior

In this section, we apply the results from the perturbation analysis to summarize the global behavior of the nonlinear QP Mathieu equation (with $\omega_1 = 1$ and $\omega_2 = \omega$), as a function of parameter values, in relation to the linear system. The parameter, ε, is assumed fixed and restricted to small values. Conclusions are valid through $\mathcal{O}(\varepsilon)$. Consequently, there exists an exceptional set of parameter points (δ, ω) for which the following summary does not apply. However, such points are exceptional in the sense that the corresponding area of parameter space is of $\mathcal{O}(\varepsilon^2)$.

For both the linear and nonlinear systems, regions of instability (i.e., unstable origin) associated with 2:1 resonances between the respective driving frequencies and the natural frequency of the system are, to leading order, bounded by the transition curves

$$\delta = \frac{1}{4}\omega^2 \pm \frac{1}{2}\varepsilon + \mathcal{O}(\varepsilon^2) \tag{26}$$

and

$$\delta = \frac{1}{4} \pm \frac{1}{2}\varepsilon + \mathcal{O}(\varepsilon^2). \tag{27}$$

Outside the regions of instability, the dynamics of the linear system are simple. The origin is stable and all solutions of the QP Mathieu equation

$$\ddot{x} + [\delta + \varepsilon\,(\cos \omega_1 t + \cos \omega_2 t)]x = 0, \tag{28}$$

exhibit 3-frequency QP behavior when ω_1 and ω_2 are incommensurate. In contrast, the dynamics of the nonlinear system, Equation (2), are much more complicated. Solutions may exhibit 3-frequency QP behavior, as for the linear system. However, the perturbation induces resonance bands locally in phase space which can cause the system to exhibit irregular, stochastic behavior. This is especially the case when solutions evolve in the stochastic layer that bounds the resonance band. Furthermore, the existence of subharmonic motions associated with $2m{:}1$ resonances implies that the origin is unstable for an entire class of parameter values not predicted by the linear system.

As shown in Figure 7, the transition curves given by Equations (26) and (27) partition the δ-ω parameter plane into nine disjoint regions. We shall describe the characteristic behavior of solutions of the nonlinear QP Mathieu equation in each of these regions, paying particular attention to torus breakup (emergence of a resonance band) and origin stability. This discussion is summarized pictorially in Figure 8.

5.1. Region A (Stable Origin)

To first order in ε, solutions of the linear system exhibit 3-frequency QP behavior for parameter values chosen from region A. Similarly, all solutions of the nonlinear system, as predicted by the perturbation analysis, exhibit 3-frequency QP behavior *independent* of initial conditions; subharmonic resonance with either driver is impossible for these parameter values. The absence of resonance bands, and hence the absence of irregular or stochastic motion in
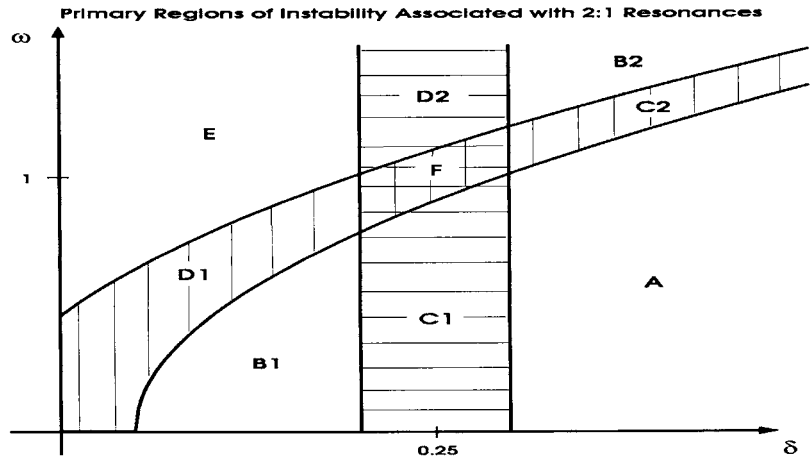
Figure 7. Primary regions of instability in the δ-ω parameter plane associated with subharmonic periodic orbits in 2:1 resonance with the two drivers, $\cos t$ and $\cos \omega t$. The parameter, ε, is fixed and set to 0.10.
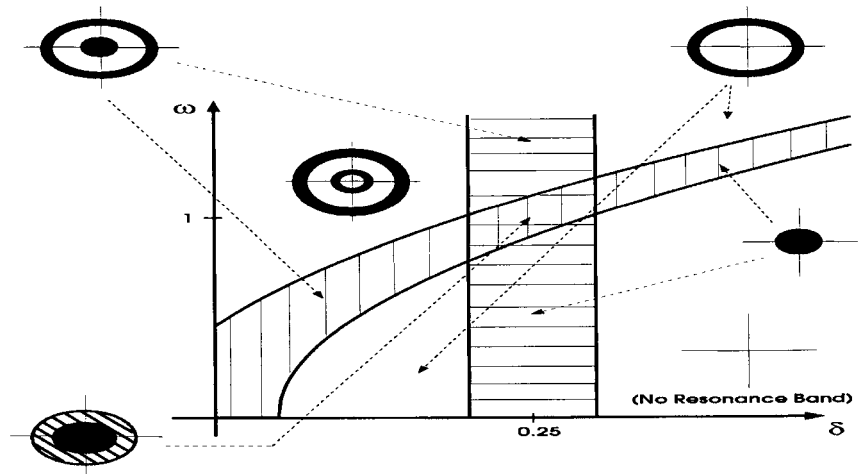

Figure 8. Schematic summary of the behavior of the nonlinear system. Resonance bands are represented by 'thick' circles.

the nonlinear system, is due to the absence of resonant tori in the unperturbed system. The condition for the existence of resonance bands associated with 2:1 subharmonic periodic orbits as determined by the resonance relation,

$$2\sqrt{\delta} \leq \omega \quad \text{and} \quad 2\sqrt{\delta} \leq 1,$$

does not hold in region A.

5.2. Regions B1 and B2 (Stable Origin)

To first order in ε, solutions of the linear system exhibit 3-frequency QP behavior for parameter values chosen from regions B1 and B2. Similarly, most solutions of the nonlinear system as predicted by the perturbation analysis exhibit 3-frequency QP behavior. However, there is exactly one resonance band in phase space associated with orbits in 2:1 resonance with one of

the two drivers – there is no resonance band associated with the other driver – and solutions with initial conditions inside the resonance band may exhibit irregular or stochastic behavior. There are periodic solutions corresponding to the equilibria in the resonance band, as well. The presence of the resonance band in phase space and the corresponding behavior of the system, due to the nonlinear resonance, are not seen or predicted in the linear system.

5.3. Regions C1 and C2 (Unstable Origin)

To first order in ε, the linear system possesses unbounded solutions for parameter values chosen from regions C1 and C2, a consequence of the instability of the origin. In the nonlinear system, however, the detuning effects from the amplitude-frequency dependence prevent unbounded behavior. This results in a resonance band surrounding and including the origin. Outside the resonance band, 3-frequency QP behavior is observed, a behavior that is not encountered in the linear system for these parameter values.

5.4. Regions D1 and D2 (Unstable Origin)

To first order in ε, the linear system possesses unbounded solutions for parameter values chosen from regions D1 and D2, a consequence of the instability of the origin. The behavior of the nonlinear system is more complicated. There are two resonance bands in phase space associated with orbits in 2:1 resonance with the respective drivers. One of the resonance bands surrounds and includes the origin, the other is bounded away from it. Solutions with initial conditions inside either resonance band may exhibit irregular or stochastic behavior but are globally bounded because of the detuning effects from the amplitude-frequency dependence. Outside the resonance bands, 3-frequency QP behavior is observed, a behavior that is not encountered in the linear system for these parameter values.

5.5. Region E (Stable Origin)

To first order in ε, solutions of the linear system exhibit 3-frequency QP behavior for parameter values chosen from region E. Similarly, most solutions of the nonlinear system as predicted by the perturbation analysis exhibit 3-frequency QP behavior. However, there are two resonance bands in phase space associated with orbits in 2:1 resonance with the respective drivers. Solutions with initial conditions inside either resonance band may exhibit irregular or stochastic behavior but are globally bounded due to the detuning. There are periodic solutions corresponding to the equilibria in the resonance band, as well. Outside the resonance bands, only 3-frequency QP behavior is observed. Although the two resonance bands are bounded away from each other, irregular motion in a large region of phase space is possible if the two bands overlap.

5.6. Region F (Unstable Origin)

To first order in ε, the linear system possesses unbounded solutions for parameter values chosen from region F, a consequence of the instability of the origin. The behavior of the nonlinear system is more complicated. There are two resonance bands in phase space associated with orbits in 2:1 resonance with the respective drivers. *Both* resonance bands surround and include the origin: solutions with initial conditions near the origin exhibit irregular or stochastic behavior, and detuning effects from the amplitude-frequency dependence prevent

unbounded behavior. Outside the resonance bands away from the origin, 3-frequency QP behavior is observed, a behavior that is not encountered in the linear system for these parameter values. The combination resonance at the origin leads to interesting dynamics, and we expect to find a complicated bifurcation scenario in this region of parameter space.

6. Conclusion

In contrast to the linear Mathieu equation,

$$\ddot{x} + [\delta + \varepsilon \cos \omega t]x = 0,$$

where instability implies unboundedness, the nonlinear Mathieu equation,

$$\ddot{x} + [\delta + \varepsilon \cos \omega t]x + \alpha x^3 = 0,$$

exhibits finite-amplitude motion as a result of nonlinear resonance. Motion is generally quasiperiodic (with two frequencies) away from the resonant orbit. However, solutions with initial conditions near the resonant orbit may exhibit local irregular or stochastic behavior – seen as chaotic – or even $2m$:1 subharmonic periodic motion corresponding to newly-emerged equilibria of an associated Poincaré map. Motion is prevented from becoming unbounded because the period-amplitude relationship resulting from the nonlinearity, αx^3, detunes the resonance: As the amplitude of motion increases, the frequency increases (if $\alpha > 0$), and the system falls out of resonance. From a dynamical systems point of view, this resonant motion carries with it a local region of phase space, which may be thought of as being separated from the rest of phase space by a separatrix surface. This view becomes increasing more accurate as $\varepsilon \to 0$ because KAM effects, which destroy invariant tori, are smaller for small ε.

In this work, we extended such considerations to the nonlinear QP Mathieu equation (2),

$$\ddot{x} + [\delta + \varepsilon (\cos \omega_1 t + \cos \omega_2 t)]x + \alpha x^3 = 0.$$

There are infinitely-many resonances associated with each of the forcing frequencies, and infinitely-many more associated with combinations of frequencies. Since resonances associated with a combination of driving frequencies are not visible at the $\mathcal{O}(\varepsilon)$ level of analysis of the perturbation method, we restricted our analysis to orbits in $2m$:1 or $2k$:1 resonance with a respective driver, $\cos \omega_1 t$ or $\cos \omega_2 t$. Accordingly, each of the two drivers (with incommensurate forcing frequencies) is treated as independently producing resonances, as though each were the forcing term of the nonlinear Mathieu equation. This results in two primary resonance bands, one for each driver, each carrying with it a local region of phase space.

The presence of the two resonant motions – manifested by two resonance bands in phase space – produces a transition from local chaos to global chaos. It was the goal of this work to characterize the dynamics of this process by means of Chirikov's overlap criterion, which states that the transition to global chaos will occur when separated regions of phase space associated with the individually studied finite-amplitude resonant motions overlap. Using a perturbation scheme based on Lie transforms and elliptic functions, we derived analytic expressions for the critical value of ε, as functions of δ, ω_1, and ω_2, at which subharmonic resonance bands in a Poincaré section of action space begin to overlap. We found that Chirikov's criterion gives a reasonable and predictably larger approximation for the critical value of ε when compared to numerical simulation of the nonlinear QP Mathieu equation. Also, we were able to characterize regions of the δ-ω parameter plane in which there is no such transition

because only one of the two resonant motions is present (cf. Regions B1, B2, C1, and C2 of Figure 7). Moreover, we found that there is a region of parameter space in which Chirikov's criterion is inappropriate because both resonant motions lie in an overlapping region of phase space even for small ϵ (cf. Region F in Figure 7).

References

1. Byrd, P. F. and Friedman, M. D., *Handbook of Elliptic Integrals for Scientists and Engineers*, Springer-Verlag, New York, 1971.
2. Chirikov, B. V., 'A universal instability of many-dimensional oscillator systems', *Physics Reports* **52**, 1979, 263–379.
3. Guckenheimer, J., Myers, M., Wicklin, F., and Worfolk, P., *dstool: A Dynamical System Toolkit with an Interactive Graphical Interface*, Department of Applied Mathematics, Cornell University, Ithaca, NY, 1991.
4. Mason, S. and Rand, R., 'On the torus flow $y\prime = a + b \cos y + c \cos x$ and its relation to the quasiperiodic Mathieu equation', in *Proceedings of the 1999 ASME Design Engineering Technical Conferences, 17th Biennial Conference on Mechanical Vibration and Noise*, Las Vegas, NV, September 12–15, 1999, Paper No. DETC99/VIB-8052 (CD-ROM).
5. Rand, R., Zounes, R., and Hastings, R., 'Dynamics of a quasiperiodically forced Mathieu oscillator', in *Nonlinear Dynamics: The Richard Rand 50th Anniversary Volume*, A. Guran (ed.), World Scientific, Singapore, 1997, pp. 203–221.
6. Zounes, R., 'An analysis of the nonlinear quasiperiodic Mathieu equation', Ph.D. Dissertation, Center for Applied Mathematics, Cornell University, Ithaca, NY, 1997.
7. Zounes, R. and Rand, R., 'Subharmonic resonance in the nonlinear Mathieu equation', *International Journal of Non-Linear Mechanics* **37**(1), 2001, to appear.
8. Zounes, R. and Rand, R., 'Transition curves for the quasiperiodic Mathieu equation', *SIAM Journal on Applied Mathematics* **58**, 1998, 1094–1115.